# The Use of an Automated Nowcasting System to Forecast Flash Floods in an Urban Watershed

HATIM O. SHARIF*

*Lawrence Berkeley National Laboratory, Berkeley, California, National Center for Atmospheric Research, Boulder, Colorado, and Princeton University, Princeton, New Jersey*

DAVID YATES

*National Center for Atmospheric Research,+ and Department of Civil Engineering, University of Colorado, Boulder, Colorado*

RITA ROBERTS AND CYNTHIA MUELLER

*National Center for Atmospheric Research, Boulder, Colorado*

(Manuscript received 19 January 2005, in final form 16 May 2005)

ABSTRACT

Flash flooding represents a significant hazard to human safety and a threat to property. Simulation and prediction of floods in complex urban settings requires high-resolution precipitation estimates and distributed hydrologic modeling. The need for reliable flash flood forecasting has increased in recent years, especially in urban communities, because of the high costs associated with flood occurrences. Several storm nowcast systems use radar to provide quantitative precipitation forecasts that can potentially afford great benefits to flood warning and short-term forecasting in urban settings. In this paper, the potential benefits of high-resolution weather radar data, physically based distributed hydrologic modeling, and quantitative precipitation nowcasting for urban hydrology and flash flood prediction were demonstrated by forcing a physically based distributed hydrologic model with precipitation forecasts made by a convective storm nowcast system to predict flash floods in a small, highly urbanized catchment in Denver, Colorado. Two rainfall events on 5 and 8 July 2001 in the Harvard Gulch watershed are presented that correspond to times during which the storm nowcast system was operated. Results clearly indicate that high-resolution radar-rainfall estimates and advanced nowcasting can potentially lead to improvements in flood warning and forecasting in urban watersheds, even for short-lived events on small catchments. At lead times of 70 min before the occurrence of peak discharge, forecast accuracies of approximately 17% in peak discharge and 10 min in peak timing were achieved for a 10 km$^2$ highly urbanized catchment.

## 1. Introduction

Hydrologic modeling of urban flood potential has witnessed an upsurge in interest recently (e.g., Ogden et al. 2000; Lee and Heaney 2003; Zhang and Smith 2003) because the hydraulic properties of these areas, such as large expanses of impervious areas, smoothed and compacted land surfaces, and modification of natural flow paths, create conditions suitable for reduced infiltration, storage, and friction losses, creating conditions favorable to high-peak flow responses. The probability of flooding from a given storm is typically higher in urban areas (e.g., Konrad and Booth 2002); a striking example is that on the same evening of the flash flood that devastated Fort Collins, Colorado, on 27 July 1997, a more intense storm occurred in rural Colorado with no reported injuries or significant damage (M. Kelsch 2003, personal communication). Simulation and prediction of floods in complex urban settings requires distributed precipitation estimates and distributed hydrologic modeling.

* Current affiliation: University of Texas at San Antonio, San Antonio, Texas.

+ The National Center for Atmospheric Research is sponsored by the National Science Foundation.

*Corresponding author address:* Dr. Hatim Sharif, Civil and Environmental Engineering Dept., University of Texas at San Antonio, 6900 N. Loop 1604 W., San Antonio, TX 78249.
E-mail: hatim.sharif@utsa.edu

The need for reliable flash flood forecasting has increased in recent years, especially in urban communities, because of the high costs associated with flood occurrences; in the United States, an average of 100 people lose their lives in floods annually, with flood damage averaging more than $2 billion (see htpp://www.noaa.gov/floods.html). A number of flood control districts, including that of Denver, Colorado, use the Automated Local Evaluation in Real-Time (ALERT) method developed in the 1970s by the National Weather Service. The ALERT system continues to provide valuable early flood detection and decision support for several urban communities, including the Denver area, with more than 140 gauging stations. ALERT systems depend mainly on automated rain gauge networks that can provide rainfall estimates in near–real time by radio telemetry. However, the densities of these networks are typically not fine enough for accurate flash flood forecasting (Bedient et al. 2003). Another problem with rain gauge networks is that they are subject to degraded levels of accuracy with increased precipitation intensities, such as those associated with flood-producing storms. In addition, gauge-based storm data are less useful in real-time storm tracking compared to those of radar.

The Weather Surveillance Radar-1988 Doppler (WSR-88D) Next Generation Weather Radar (NEXRAD) is capable of detecting precipitation at a resolution and areal extent previously impossible with traditional rain gauge networks and has brought unprecedented advances in estimating areally distributed, real-time rainfall data for both hydrologic and hydrometeorological applications, including flood warning and forecasting (National Research Council 1996). In addition to the high temporal and spatial resolution of the radar-rainfall data, an equally important factor in the future utility of radar-rainfall data for operational use in urban hydrology is the cost savings that may arise from the use of radars over rain gauge networks (Tilford et al. 2002). Moreover, several nowcast systems use radar to provide quantitative precipitation forecasts (Wilson et al. 1998) that can potentially afford great benefits to flood warning and short-term forecasting in urban settings.

Nowcasts are typically defined as short-time and space-specific forecasts of periods less than a few hours, and may include storm initiation, growth, dissipation, and storm features such as wind speeds and direction and precipitation rates. Some of these nowcast systems employ gridded radar data for storm analysis and trending and to extrapolate storms positions (Mueller et al. 2003). Examples of this type are the Thunderstorm Identification, Tracking, Analysis, and Nowcasting (TITAN) algorithm (Dixon and Wiener 1993) and the Strom Cell Identification and Tracking algorithm used by the National Severe Storm Laboratory's Warning Decision Support System (Johnson et al. 1998). More complex nowcast systems employ radar data in combination with meteorological observations, numerical weather prediction, and feature-detection algorithms to nowcast storm evolution. Examples of these sophisticated systems that are used operationally include the Federal Aviation Administration Regional Convective Weather Forecast and Terminal Weather Convective Forecast System (Boldi et al. 2002) and the Auto-Nowcaster (ANC) system developed at the National Center for Atmospheric Research (NCAR) (Mueller et al. 2003). The ANC is the nowcast system used in this study, which makes use of multiple data ingest products (gridded radar fields, surface mesonet data, sounding data, etc.) to produce, among other things, 0–60-min quantitative precipitation nowcasts.

The overall objective of this study is to demonstrate the potential benefits of high-resolution weather radar data, physically based distributed hydrologic modeling, and quantitative precipitation nowcasting for urban hydrology and flash flood forecasting. Radar reflectivity data from WSR-88D radar and forecast fields are used to compute high-resolution rainfall estimates that are input to a state-of-the-art physics-based distributed-parameter hydrologic model to forecast flooding over a small, highly urbanized catchment in Denver. Two rainfall events that occurred on 5 and 8 July 2001 in the Denver region, during which the ANC system had been operated, are presented. The observed rainfall and streamflow data on 8 July were used to validate the hydrologic model. Simulations driven by rain gauge and radar-rainfall estimates are compared to highlight the benefit of distributed rainfall information. Nowcasts for both events were used to evaluate the ability of ANC to produce rainfall nowcasts that are useful for urban hydrologic analysis and forecasting. Hydrologic model outputs using nowcast precipitation fields were compared to outputs produced using the radar-rainfall estimates, which were assumed to be the best available rainfall information.

## 2. The hydrologic model

The Gridded Surface Subsurface Hydrologic Analysis (GSSHA) model (Downer and Ogden 2004) is a physically based distributed-parameter hydrologic model. GSSHA is a reformulation and enhancement of the finite-difference Cascade Two-Dimensional (CASC2D) model (Ogden 2000) that simulates infiltration-excess (Hortonian) runoff. It extends CASC2D to allow the subsurface water components of the hydro-

logic balance, both saturated and unsaturated zones, to be included in watershed simulations. GSSHA simulates two-dimensional overland flow, one-dimensional channel routing, rainfall distribution, canopy interception, microtopography, infiltration, and evapotranspiration using finite-difference and finite-volume methods. Additionally, GSSHA uses a one-dimensional finite-difference solution of Richards' equation to simulate the unsaturated zone. GSSHA operates on a digital elevation model of the watershed using square grids that typically range from 10 to 1000 m on a side.

Infiltration into the soil is optionally modeled using either the Green and Ampt (1911) method, or the Green and Ampt redistribution method (Ogden and Saghafian 1997). This infiltration technique is similar to the method described by Smith et al. (1993), with the assumption of rectangular soil moisture profiles and the addition of an analytically derived unsaturated capillary head term (Ogden and Saghafian 1997). The infiltration option allows accurate simulation of infiltration when there are multiple ponding periods. The original Green and Ampt (1911) equation is expressed in GSSHA as:

$$f = K\left[\frac{H_c(\theta_e - \theta_i)}{F} + 1\right], \tag{1}$$

where $f$ is the infiltration rate (L/T), $K_s$ the soil saturated hydraulic conductivity (L/T), $H_c$ the Green and Ampt capillary head term (L), $\theta_e$ the soil effective porosity (dimensionless), $\theta_i$ the soil initial water content (dimensionless), and $F$ the cumulative infiltrated depth (L).

GSSHA also provides detailed modeling of the soil water profile in the unsaturated zone. It solves the one-dimensional (in the vertical direction) head-based form of Richards' equation,

$$C(\psi)\frac{\partial\psi}{\partial t} - \frac{\partial}{\partial z}\left[K(\psi)\left(\frac{\partial\psi}{\partial z} - 1\right)\right] - W, \tag{2}$$

where $C$ is the specific moisture capacity, $\psi$ soil capillary head (L), $z$ vertical coordinate (downward positive) (L), $t$ time (T), $K(\psi)$ effective hydraulic conductivity (L/T), and $W$ a source/sink term (L/T). The head-based formulation allows for the solution of Richards' equation in both saturated and unsaturated conditions (Haverkamp et al. 1977). Either the Brooks and Corey (1964) equations, as extended by Hutson and Cass (1987), or the Haverkamp et al. (1977) equations, as modified by Lappala et al. (1987), can be used to define the soil pressure ($\psi$)–water content ($\theta$), $\psi$–hydraulic conductivity ($K$), and $\psi$–water capacity ($C$) relationships. The implicit solution to Richards' equation is first-order accurate in time and second-order accurate in space. Flux updating, as described by Kirkland (1991), is used to ensure mass conservation. Iterations can also be used to improve accuracy and mass balance. Internal time step limitations, as described by Belmans et al. (1983), also help keep the model stable, accurate, and mass conserving.

Once ponding occurs on a grid cell, surface water is accumulated until the specified retention depth of the cell is exceeded. Thereafter, the overland flow is routed in two orthogonal directions using Manning's equation with the diffusion waveform of the de St. Venant equations to estimate friction slope. When the overland flow reaches a model grid cell that is specified as a channel cell, the flow is passed into the channel and routed using a one-dimensional routing technique.

## 3. The 8 July 2001 flood event

The 2001 flood season in Denver was above average in terms of the number of flood messages issued by the Flood Control District. The week of 14 July was particularly wet with flash flood warnings issued on 3 days (8, 10, and 13 July) and flash flood watches for three others. The 8 July storm event produced the worst flooding of the year because flash flooding was observed on several watersheds, including the Harvard Gulch, and along a major highway. Annual peaks were recorded by 16 stream gauges, with 5 breaking their historic marks. Harvard Gulch experienced a record flood with much of the upper basin receiving more than 3 in. of rain. In this study, the flooding of Harvard Gulch is simulated to validate the distributed modeling approach for this type of watershed. Several specific tasks are required: acquiring and processing radar-rainfall data for the event from the Denver WSR-88D radar archived level II data, acquiring rainfall observations from five U.S. Geological Survey (USGS) rain gauges located in or very close to Harvard Gulch, and using the rainfall data as input to GSSHA to simulate the 8 July flood.

### *a. Rainfall data*

Rainfall observations from five tipping-bucket rain gauges operated by the USGS were obtained (bucket size of 0.01 in.; see Fig. 1).

The Denver WSR-88D radar is located about 40 km from the watershed and operated continuously during the 5 and 8 July cases. Rainfall was estimated from the three-dimensional volume scan reflectivity fields using the National Weather Service default relationship between the radar reflectivity $Z$ ($\text{mm}^6\ \text{m}^{-3}$) and the rainfall rate $R$ ($\text{mm}\ \text{h}^{-1}$):

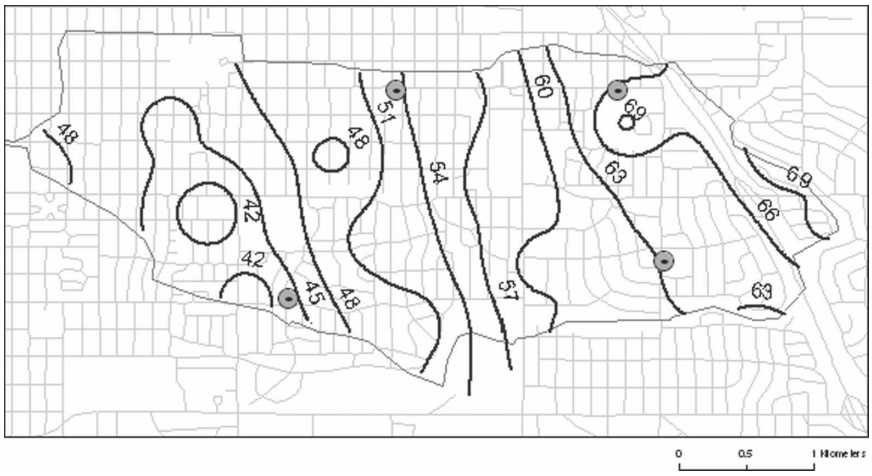


FIG. 1. The Harvard Gulch watershed, storm-total radar-estimated rainfall, and location of USGS rain gauges. The street networks of the urban area are shown in the background.

$$R = aZ^b. \quad (3)$$

The values of $a$ and $b$ in Eq. (3) are $a = 0.017$ and $b = 0.714$. These parameters correspond to the relation $Z = 300R^{1.4}$ (Battan 1973). This is the relationship typically applied by the National Weather Service for this radar (Fulton 1999). Also, for this radar a rain-rate threshold (also called the *hail cap*) of 74.7 mm $h^{-1}$ is specified by the National Weather Service (Fulton et al. 1998; Fulton 1999). Rain rates are capped at this value to prevent hail contamination associated with convective storms, which can significantly enhances radar reflectivity values. All reflectivity values above 51 dB$Z$ (which corresponds to the rain rate of 74.7 mm $h^{-1}$) were assumed to have been a result of hail presence and were reset to 51 dB$Z$ [radar reflectivity is usually expressed in decibels of $Z$, that is, dB$Z$, where dB$Z = 10 \log_{10}(Z)$]. On the other hand, all reflectivity values below 25 dB$Z$ are assumed to be the result of clear-air return not associated with rainfall and were eliminated. Radar-rainfall data are then used without further adjustments. The radar-rainfall field has a 5–6-min temporal resolution and a special resolution of 1 km $\times$ 1°.

### b. Watershed characteristics

The Harvard Gulch (Fig. 1) has an area of approximately 10.2 $km^2$ of mixed urban land use and is twice as long as it is wide. A 30-m grid size was found sufficient to describe the topography and land surface features of the watershed. Topography and land use/cover data were obtained from the USGS digital database (Earth Resources Observing Systems Data Center, National Elevation Data and National Land Cover Data information available online at http://ned.usgs.gov and http://landcover.usgs.gov, respectively). Land use/cover features were modified based on information obtained from the Denver Urban Drainage and Flood Control District and a site visit. General terrain slope of the catchment is from east to west with local slope values ranging from 0.5 to 2%. Base flow is typically less than 0.12 $m^3 s^{-1}$. Impervious areas cover about 40% of the watershed, while soils in the watershed are classified as the Soil Conservation Service Group B. The Harvard Gulch is heavily channelized and is drained by a combination of trapezoidal, rectangular, and closed-conduit channels. Details of the channel cross sections and properties were also provided by the Flood Control District.

### c. Hydrologic model validation

A number of studies discussed the effects of spatial variability in watershed characteristics on the hydrologic response. Woolhiser (1996) showed that infiltration-excess runoff, typically associated with urban and semiarid catchments, is strongly influenced by the spatial variability of soil hydraulic conductivity. Merz and Plate (1997) demonstrated that the effect of spatial variability, which is typically large for midsized events, decreases for very small and very large events. Ogden et al. (2000) reached similar conclusions when they analyzed the July 1997 flash flood in Fort Collins.

The GSSHA model was used to simulate the spatially varied hydrologic response of Harvard Gulch on 8 July. The simulation was simplified for two reasons. First, it is assumed that runoff from the storm is essentially generated by the infiltration-excess mechanism. Because of the semiarid climate and the low soil hydraulic conductivity (the dominant soil type is silty loam), lateral sub-

surface flow and saturation from below resulting from the rising of the water table for this short, high-intensity storm is likely insignificant. Second, no complex hydraulic structures exist in the simulated catchment. Nonetheless, we included as much detail of the land surface features and the drainage system as was available.

Soil hydraulic properties are available from the Natural Resources Conservation Service county map. Because those are approximate values, we used values computed through calibration for the Fort Collins flood (Ogden et al. 2000) where similar soil properties exist. We used the same parameters used in Fort Collins for identical soil types because the two watersheds are located in the same region and topography and the climatology are similar. Moreover, sensitivity experiments indicate that even a factor of 2 change in soil hydraulic conductivity does not have a significant effect on the runoff hydrograph driven by heavy precipitation for this catchment (H. O. Sharif et al. 2003, unpublished manuscript). There are two dominant soil types: silty loam covers about 60% of the watershed and the remainder is impervious. Silty loam is assigned a mean saturated hydraulic conductivity (K) of 0.34 cm $h^{-1}$, a mean effective porosity of 0.5, and a mean capillary head of 16.7 cm. The values of the hydraulic parameters are randomly varied around the means to account for soil heterogeneity. Computed percent imperviousness for 33 subareas within the Harvard Gulch was obtained from the Denver Flood Control District. Impervious model grid cells within these subareas are distributed randomly to represent the specified percentages. In some cases, impervious cells are aligned along major streets – the size of the model cell is 30 m. Values for overland flow roughness coefficients were obtained from published sources (Soil Conservation Service 1986; Ogden et al. 2000) and are listed in Table 1. Retention depth is assumed to be a function of land use, and values were assigned following Tholin and Keifer (1960). Retention depths for different land use/cover types are also listed in Table 1. Previous applications of the model showed that the value of the retention depth has some effect on the runoff volume and hydrograph shape (e.g., Ogden et al. 2000). Unlike hydraulic properties, which were stochastically distributed, we assigned constant values of the roughness coefficient (or retention depth) for each land use/cover type. After vigorous sensitivity testing on a watershed where the Hortonian runoff was dominant, Ogden and Dawdy (2003) concluded that for big rainfall events the initial soil moisture state can have a significant effect, but only if the soils are extremely wet or dry, that is, a significant difference between results if one assumes extremely wet initial conditions for actually extremely dry initial conditions. Merz and Plate (1997) also downplayed the impact of soil moisture variability for the case of large events. There were some rainfall events in the weeks before this event but no events since 5 July. Certainly, the watershed was not very dry, and given the temperature of 5–8 July it is very unlikely that the watershed was still extremely wet on 8 July. We used an intermediate value of initial soil moisture to minimize the effect on our results.

TABLE 1. Model parameters for different land use/cover types.

| Land use/cover type | Manning roughness coefficients | Retention storage (mm) |
|---|---|---|
| Impervious areas | 0.02 | 1.3 |
| Industrial | 0.15 | 1.4 |
| Public areas | 0.20 | 1.4 |
| Residential (lawns) | 0.20 | 5.0 |

Rainfall data from the WSR-88D radar and five USGS rain gauges were used as input to the hydrologic model. No calibration was done at this stage. Unfortunately, the USGS stream gauge at the watershed outlet stopped recording 15 min after the beginning of the 8 July event because of the discharge intensity. Consequently, there are only three points on the actual outlet hydrograph that are comparable with the hydrograph simulated by the model.

Information from the stream gauge operated by the Flood Control District was not of much help because of the effects of a detention basin and the inflow from another watershed (Dry Creek) that merges with the Harvard Gulch channel between the two stream gauges. Figure 2 shows that simulation results based on

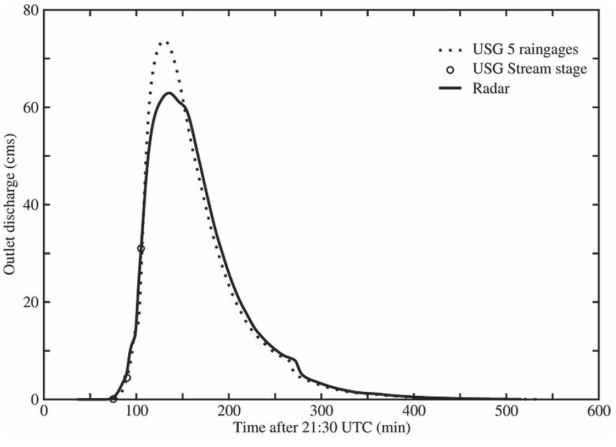


FIG. 2. Simulated runoff hydrographs driven by radar and rain gauge estimates. Available USGS stream gauge measurements are shown (open circles).

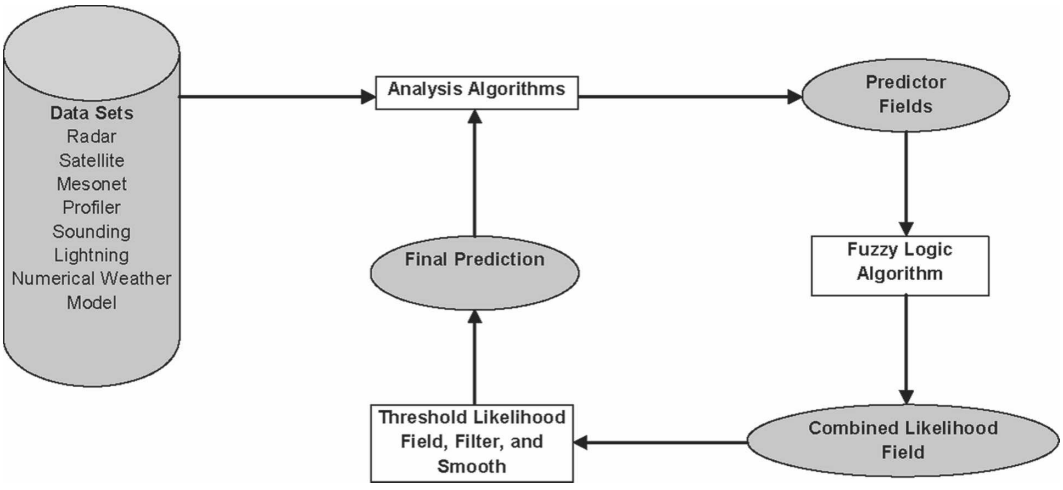


FIG. 3. Simplified schematic of the ANC system.

radar and rain gauge data match discharge values recorded by the USGS stream gauge both in terms of timing and magnitudes. The inverse-distance method is used to construct rain fields from rain gauge data. The peak discharge computed using rain gauge data is higher than the one computed using radar data by 20%, although there is no difference in timing.

The authors learned that USGS subsequently estimated a peak discharge of 2040 cfs at the Harvard Gulch Park gauge based on their high-water marks field survey, which is less than our estimated peak discharge based on radar rainfall by about 9% (K. Stewart, Denver Urban Drainage and Flood Control District official, 2004, personal communication). This makes us more confident about the simulation results, especially when radar data are used, having accurate simulation of the rising limb of the hydrograph reasonable estimate of the peak discharge. The total accumulated precipitation from the event is virtually the same using radar or gauge information. One has to be cautious about suggesting that radar-rainfall data are better for this case because radar estimates can be biased for one reason or another. The radar estimates have spatially and temporally variable errors even if the mean bias is eliminated; Sharif et al. (2002) demonstrated examples of such cases.

## 4. The NCAR ANC

The Auto-Nowcaster used in this study is a software system that combines output from feature-detection algorithms and thunderstorm extrapolation/trending software in a "data fusion" system to produce short-term 0–1-h thunderstorm forecasts (nowcasts). A simplified schematic of the ANC system is provided in Fig. 3. The steps in producing the nowcast are briefly reviewed here to give an overview of the entire system.

The system receives operational meteorological data from several sources, including radar (mainly WSR-88D), satellite, surface stations (including special mesonets), lightning, profilers, numerical weather model, and radiosondes. The first step in producing the nowcast is running a group of analysis algorithms on these datasets to calculate predictor storm fields. Analysis algorithms include data quality control routines, TITAN, and a Tracking Radar Echoes by Correlation algorithm (Tuttle and Foote 1990) that retrieves the three-dimensional wind speed and direction, and a numerical boundary layer model and its adjoint (Variational Doppler Radar Analysis System; Sun and Crook 2001).

A major feature of ANC is its ability to use this boundary layers model and other feature-detection algorithms to identify and characterize the boundary layer. It is possible for a forecaster to interact with ANC by manually inputting the position of boundaries in an optional intermediate step. The predictor fields developed in the first step are combined using a fuzzy logic approach. The fuzzy logic approach uses membership functions to map the predictor fields to the likelihood of storms (likelihood fields). The dimensionless likelihood fields are meant to represent the relationship between the predictor fields and the existence of convective storms at validation time. The likelihood fields are weighted and summed to produce a combined likelihood field. The combined likelihood field is filtered and thresholded in a third step to generate the nowcast areas of convective activity.

In ANC deployments to date, the automated now-

casts are used as guidance by the forecasters. The major advantage of ANC is its ability to forecast storm, initiation, growth, and dissipation. For this application, the simulated new reflectivity fields are converted to rain rates using the WSR-88D $Z$–$R$ relationship.

As with virtually all automated nowcast systems, the existence of mountains imposes a serious challenge on utilizing the full capabilities of the ANC system. TITAN is less affected by the complex terrain and is used to detect and extrapolate the position of existing thunderstorms. TITAN uses three-dimensional Cartesian radar data as input. It employs a centroid-based methodology for identifying storms as objects and matching these objects to those at a subsequent time to produce storm-track information. Based on past storm trends, TITAN predicts future storm location and size. Products from TITAN are input into the Auto-Nowcaster and provide information on storm size, movement, and trend. The TITAN algorithm does not rely on boundary layer winds and can be used in mountainous terrain. This algorithm, along with satellite-based algorithms, is the major component of the Auto-Nowcaster that are typically employed in complex terrain when boundary layer winds are not obtainable.

Outputs from all of the various algorithms described above are combined by the Auto-Nowcaster system to produce nowcasts every 5–6 min of thunderstorm initiation, growth, decay, and movement. Nowcasts using the full capacity of the ANC and nowcasts based on TITAN extrapolations will be used in this study to highlight the differences between the two approaches. The hydrologic model will be used to simulate runoff hydrographs based on the ANC nowcast for 2 days in July 2001.

## 5. Examples of rainfall nowcasting

The ANC nowcast of two storm events that produced significant rainfall in the Denver metropolitan area are demonstrated. The 5 July 2001 storm represents a case where the ANC produced reasonably accurate nowcasts. On 8 July 2001, flash flooding occurred from storms over the Denver urban area, but the performance of the ANC was limited because of the presence of complex terrain located approximately 60 km west of Denver. Given the difference in the performance of ANC during these two events, the main motivation for studying these cases is to evaluate the hydrologic forecasts based on these nowcasts. A brief description of the meteorological synoptics of these storms and a discussion of the ANC results are provided below.

### *a. 5 July 2001 case*

Mueller et al. (2003) provided a detailed review of this case. Here, a short summary is presented. On 5 July, synoptic-scale forcing over Colorado was weak. The steering-level winds were approximately 5 m $s^{-1}$ from the southeast. Surface dewpoints were ~10°C, which is typical of values observed on days when thunderstorms occur in the Denver area in the summer convective season. Storms initiated, grew, and dissipated within the radar domain over a 2.5-h period. The storms were located approximately 40 km east of the foothills of the Rocky Mountains near the Denver International Airport. In this region, the Denver WSR-88D has a strong signal from clear-air return and the boundary layer is well defined. Figure 4b shows an example a 60-min ANC precipitation rate nowcast. The radar reflectivity at nowcast time is shown in Fig. 4a. The 60-min nowcast predicts storm initiation and growth (as indicated by an increased area of convection in the nowcast). In this case, boundary layer convergence fields associated with the collision of multiple boundaries were the main contributors to the nowcast. Figure 4c shows the radar reflectivity at validation time. The ANC nowcast compares well with the observations. Later in the time period, the dissipation of the system is also handled well by the ANC. This is a case demonstrating the performance of the ANC when information about the early growth of storm was available. The performance is typical for cases when all data needed are available and full capabilities of the ANC can be utilized.

### *b. 8 July 2001 case*

This is a case when topography limits the amount of information available for the ANC especially early in the growing stage of the storm. On 8 July 2001, storms developed in the early afternoon over the Rocky Mountains, located approximately 60 km west of the center of the Denver metropolitan area. The more intense thunderstorms, gust fronts, and associated convergence boundaries moved off the foothills and propagated toward Denver at 2200 UTC. One thunderstorm outflow located SW of Denver was particularly intense, initiating new storm development by 2230 UTC as it moved toward Denver. The new storms (see Fig. 5a) grew rapidly over a 30-min period and produced heavy precipitation, hail, and flash flooding over portions of the Denver urban area and at several of the Denver streams by 2300 UTC (Fig. 5b). The areal extent of precipitation rain rates $>100$ mm $h^{-1}$ essentially doubled during the 30-min period shown in Figs. 5a,b. Both TITAN and the Auto-Nowcaster ran in real time

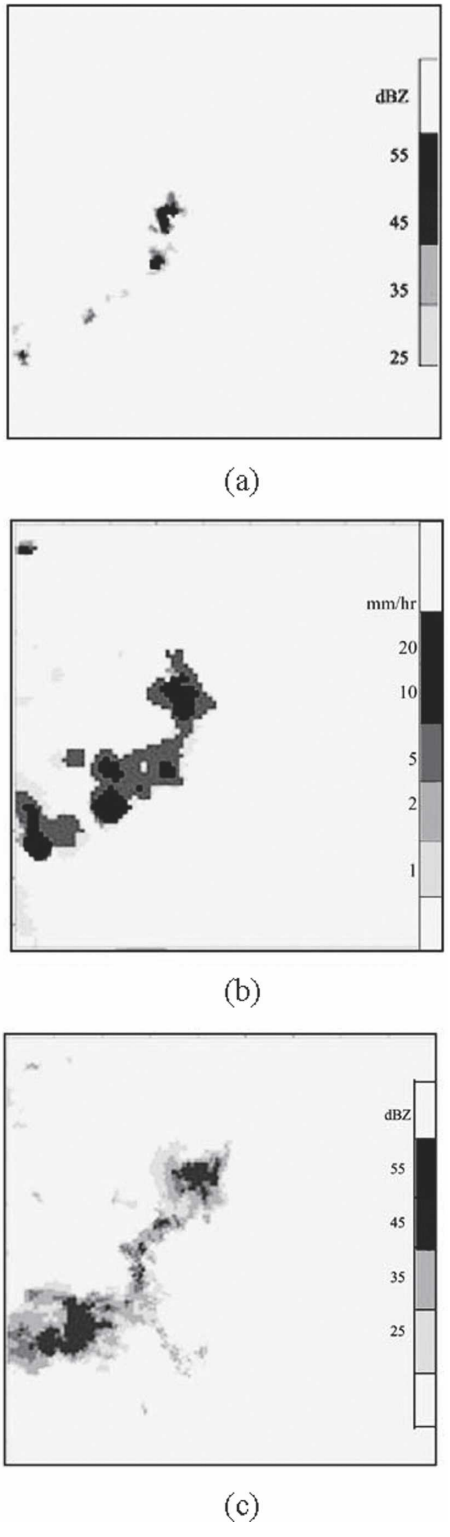


FIG. 4. An example ANC precipitation rate nowcast for the 5 Jul event: (a) reflectivity at forecast time (dB$Z$), (b) 60-min forecast of rainfall rate (mm h$^{-1}$), and (c) reflectivity at valid time for 60-min forecast (dB$Z$).

on 8 July. The Auto-Nowcaster produced 30- and 60-min nowcasts of rain rate at 6-min intervals during the evolution of this event.

The 30-min storm extrapolation (TITAN) rainfall rates compared relatively well to the gauge rain rates during the first 30 min of the flash flood event, with differences of 20%–30% observed in *peak* magnitudes between the gauge measurements and extrapolated storm rain rates. The ANC 30-min rain-rate nowcasts showed some improvement over the extrapolation rain rates throughout the flash flood event. The difference in performance between ANC nowcasts and TITAN extrapolations can be seen in Figs. 5c,d at the time of peak rainfall at 2300 UTC. While there is not a major difference in the two rain-rate plots, it can be seen that the ANC nowcasts provide a better representation of the larger areal extent of the $>100$ mm h$^{-1}$ rain rates that actually occurred (see Fig. 5b). This is because the Auto-Nowcaster is able to provide nowcasts of storm growth and decay, in addition to nowcasting the initiation of new storms—a capability that does not exist within extrapolation techniques such as TITAN. The Auto-Nowcaster system relies on the *timely* detection of both a surface convergence boundary and the detection of clouds growing aloft, above the boundary, in order to produce accurate 30-min nowcasts of rainfall rate. The complex terrain of the Rocky Mountains located upstream of Denver prevented early observation of the thunderstorm outflows and of the rapid growth of the storms 15 min prior to their impact on the Harvard Gulch basin. Thus, longer-period nowcasts failed to capture storm initiation and predict the intensification of outflows, which is crucial to nowcasting the rapid intensification of storms.

## 6. Runoff predictions based on rainfall nowcasts

Rainfall estimates and nowcasts for the 5 and 8 July events were used as inputs to the GSSHA model to compute corresponding runoff nowcasts. The nowcast precipitation fields have roughly the same spatial and temporal resolutions as the radar estimates used to produce them—1-km grids at 5–6-min intervals. The nowcast rainfall fields are generated at lead times of 30 and 60 min. Hydrographs for the events computed using radar estimates directly are assumed to be the references against which hydrographs driven by the nowcast precipitation fields are compared; note that the former have a 5–6-min temporal resolution and a 1 km $\times$ 1° spatial resolution.

The hydrologic model was run first with rainfall inputs from the ANC for the 5 July event to evaluate the accuracy of the simulated hydrologic forecasts. As men-

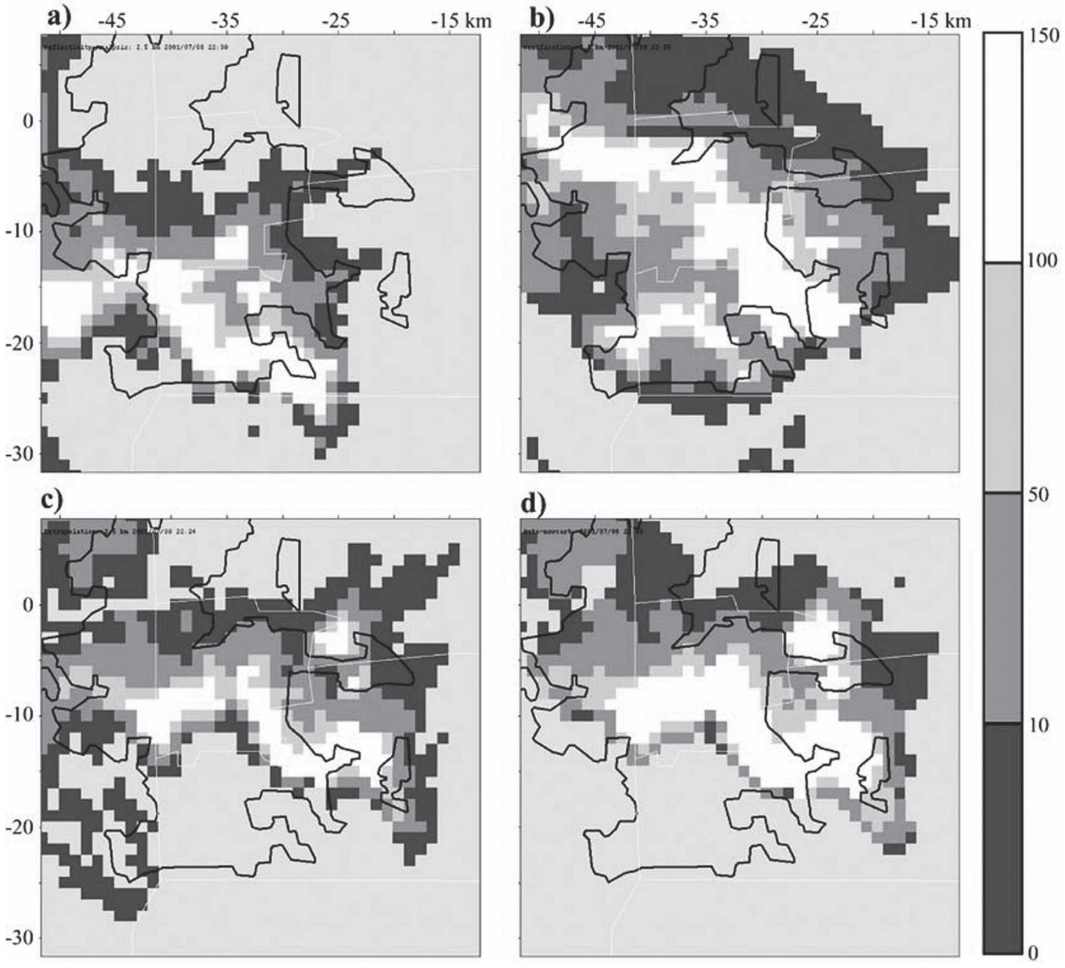


FIG. 5. An example ANC precipitation rate nowcast for the 8 Jul event: (a) precipitation rate at forecast time (mm $h^{-1}$) (2230 UTC), (b) observed precipitation rate (mm $h^{-1}$) (2300 UTC), (c) TITAN forecast of (b) made at 2230 UTC, and (d) ANC forecast of (b) made at 2230 UTC.

tioned earlier, 5 July represents a case where the ANC produced reasonable nowcasts. Every 5 min the ANC generated discrete 30- and 60-min nowcasts (two values). The hydrologic model uses precipitation fields from radar estimates up to the nowcast time and the 30- and 60-min nowcasts. Because the rainfall inputs to the hydrologic model have a 5–6-min resolution, estimates for intermediate time steps were interpolated linearly from the 30- and 60-min nowcast fields. As the ANC produces new precipitation nowcasts (every 5–6 min), previous nowcast values are discarded. In Fig. 6, the lead time represents the difference between the nowcast time "now" and the time when the peak discharge occurred, as estimated using radar-observed precipitation. The error in estimating the peak discharge 70 min before the peak occurrence is about 65%. The error in runoff volume is smaller than the error in peak discharge, but the shapes of the two plots look similar. The errors in peak discharge and runoff volume do not decrease with time and have multiple spikes. One would expect that the error plotted in Fig. 6 would decrease with time if the skill of the ANC is consistent, and actually the latter is true for this experiment. But, the error values fluctuate because of the interpolation between the forecast values. Even if the forecasts are perfect, two instantaneous values cannot represent a rainfall process with high temporal variability. For some cases, for example, 55 min prior to the peak occurrence, the two values represented the rainfall variability quite well, while the two forecast values at 35 min before the peak occurrence represent two spikes in the rainfall hyetograph, and when interpolation was solely based on these two points the forecast rainfall volume was much larger than the estimates. The spatial variability also played a role in this result. We actually performed careful inspection of precipitation values on every radar

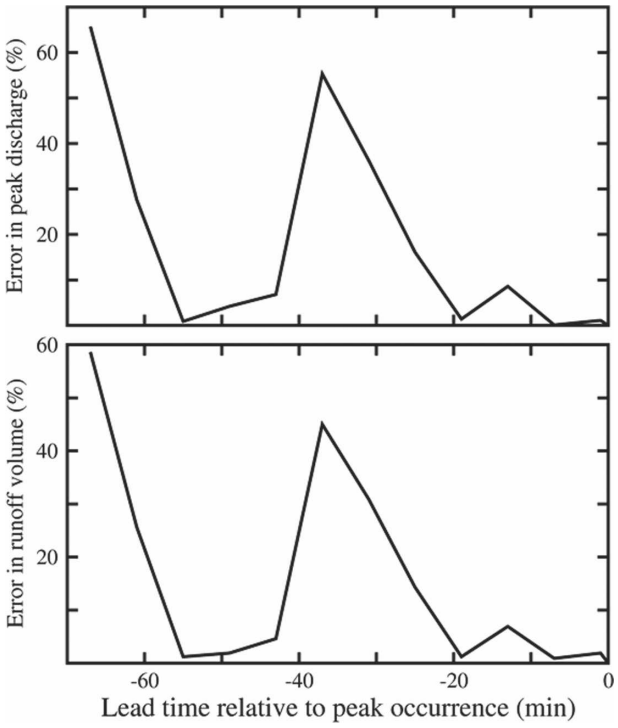


FIG. 6. Errors in the forecasted runoff as a function of the forecast lead time for the 5 Jul event (based on ANC precipitation nowcasts); only 60- and 30-min nowcast precipitation is used, values for intermediate 5-min intervals are interpolated.

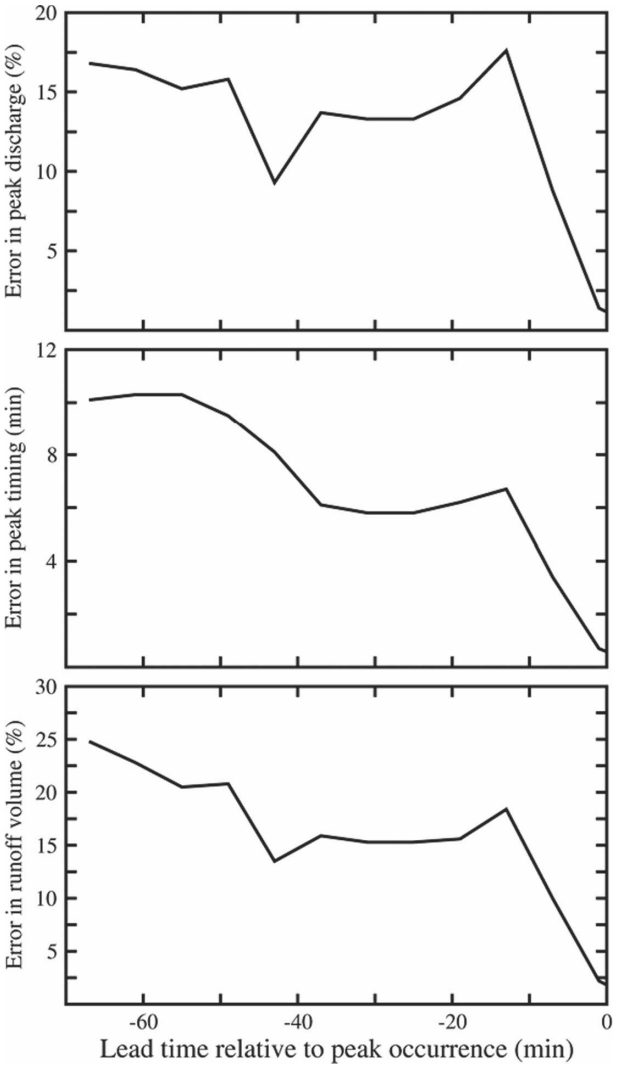


FIG. 7. Same as in Fig. 6, but previous precipitation nowcast values are also used to fill intermediate 5-min values; error in peak timing is shown in the middle panel (see text for details).

pixel for each time step to confirm this fact. This problem is similar to the problem resulting from coarse temporal resolution of radar precipitation estimates (e.g., Wilson and Brandes 1979).

In a second experiment, for the same event on 5 July, we use radar information up to the forecast time 30- and 60-min nowcast, while intermediate periods between "now" and the 30- and 60-min nowcast are filled with 30- and 60-min nowcast values from previous periods. No previous nowcast is discarded unless observed radar data become available to replace it. Use of previous nowcast values, as opposed to interpolation, considerably improves the hydrologic forecasts. This highlights the importance of temporal resolution of precipitation for this type of event. As seen in Fig. 7, the error in estimating the peak discharge, the most important hydrologic variable in flash flood nowcasting, 70 min before the peak occurrence is only about 17%. The error in peak timing is around 10 min at that time, while the error in runoff volume is about 25%. For such a small catchment the concentration time is very short and the performance of ANC would likely be better for a larger watershed where the lag time between the rainfall peak and the peak discharge is much longer. The errors in peak discharge and runoff volume decrease slightly as the lead time becomes smaller and the decrease becomes sharper 15 min before the peak occurrence.

Results of simulations using nowcast fields based only on TITAN extrapolation for the 5 July event, shown in Fig. 8, are quite different. The errors in peak discharge and runoff volume from the flood hydrographs are about 4 times as large compared to errors from the ANC fields. Errors in peak timing are twice as large compared to the ANC results with a peak at 35 min before the peak occurrence. The extrapolation errors drop to values comparable to the ANC maximum errors only 10 min before the peak occurrence. The results highlight the benefits of nowcasting storm initiation, growth, and dissipation provided by the ANC.

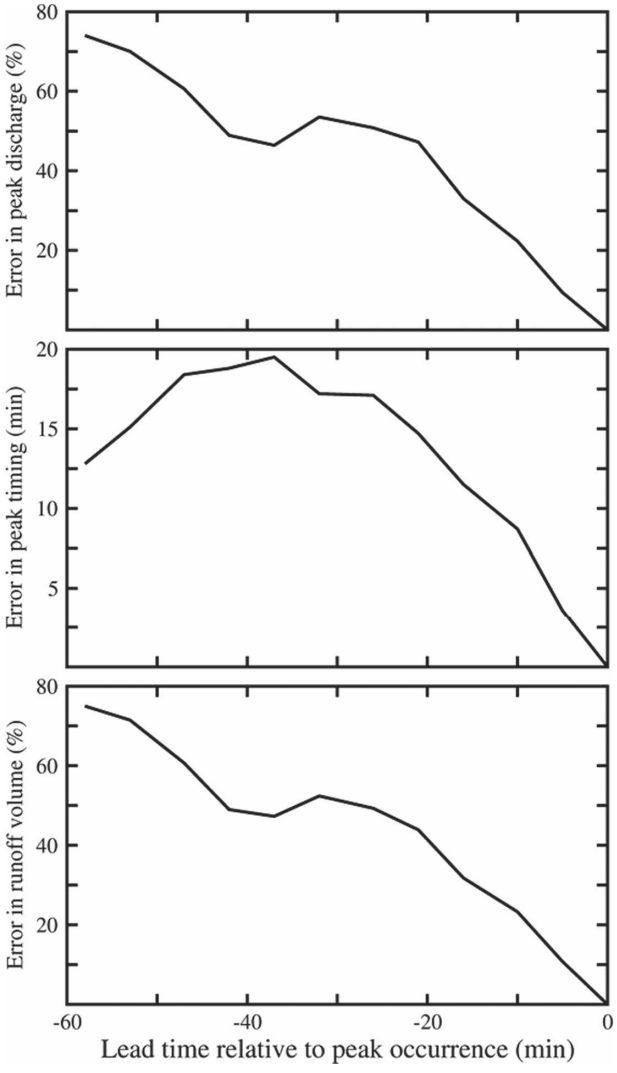


FIG. 8. Same as in Fig. 7, but precipitation nowcasts are computed using extrapolation only.

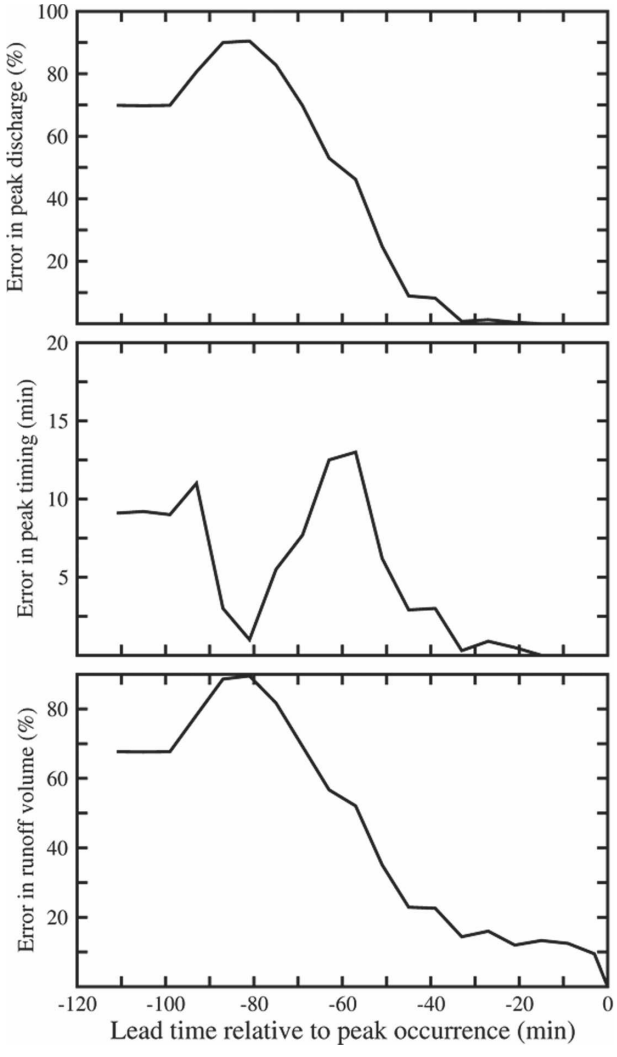


FIG. 9. Same as in Fig. 7, but results are for the 8 Jul event.

On 8 July the quality of ANC nowcasts is poorer, compared to the 5 July event, because of factors described in section 5. The hydrologic nowcasts are very poor at the beginning of the ANC runs, as shown in Fig. 9, but the errors drop very sharply for lead times less than 80 min. Interestingly, the errors in peak timing are comparable to the 5 July errors. The timing error curve shows a sharp decrease and then a sharp increase 80 min prior to the peak discharge, which is an indication of the complex relationship between hydrographs produced using different rainfall fields. As in Figs. 7 and 8, the shapes of the peak discharge and runoff volume errors are similar. The errors in Fig. 9 are smaller than the 5 July case for lead times shorter than 55 min due the difference in the watershed response to the storms. The watershed response to the 8 July storm took a longer time. This extended the time over which the hydrologic forecasts were useful.

## 7. Summary and conclusions

A preliminary attempt to simulate runoff nowcasts in a highly urbanized small catchment is presented to demonstrate the utility of advanced nowcasting techniques in urban hydrology. A physically based distributed-parameter hydrologic model is used to simulate runoff generation driven by precipitation nowcasts. The hydrologic model was first validated on the watershed using radar-rainfall estimates. Based on the limited observations available, validation indicates that there is good agreement in simulation of the rising limb of the hydrograph with a difference of 9% between simulated peak discharge and peak discharge estimate based on high water marks.

Results using the full capabilities of the ANC storm forecasting system clearly demonstrate that advanced nowcasting can lead to significant improvements in flood warning and forecasting in urban watersheds, even for short-lived events on small catchments. For the case study event typical of the performance of the ANC when needed data are available, at lead times of about 70 min before the occurrence of peak discharge, forecast accuracies of approximately 17% in peak discharge, 10 min in peak timing, and 25% in hydrograph volume were achieved for a 10 $km^2$ highly urbanized catchment. Significantly larger forecast errors resulted when only storm extrapolation was used to produce precipitation forecasts. The use of nowcast fields made at earlier time periods to fill values between the present time observations and 30- and 60-min nowcasts greatly improved the hydrologic forecasts. Even for the 8 July case, where the ANC nowcasts were not good because of a lack of meteorological information, hydrologic predictions driven by the ANC nowcasts were reasonably accurate at short lead times.

Two facts make us believe the methodology used in this study can be feasible in real-time flood forecasting. First, Harvard Gulch is a small catchment where the response to convective storms is very fast while for larger catchments the hydrologic response will be slower, allowing for a greater lead time of reliable precipitation forecast; the case of 8 July where the response was slower is a good example. For large catchments even precipitation forecasts based on simple storm translation may be very useful. Second, the complex terrain affects the performance of the ANC in the Denver area; Mueller et al. (2003) and Roberts and Rutledge (2003) presented examples where the ANC performed much better in other areas.

More studies are required before implementing an urban flash flood nowcasting system based on the tools described in this study. The hydrologic uncertainty associated with ANC outputs needs to be quantified through Monte Carlo simulations or a similar methodology. In many cases the ANC precipitation fields are reasonable in term of their magnitudes, but not so in term of their placement or orientation; the same is true for any nowcasting technique. The effects of such errors need to by analyzed, especially for small watersheds. However, radar- and ANC-based flood warning and nowcast system have the potential to provide accurate and easy-to-understand information that can be available in real time using Geographic Information Systems (GIS) and Internet technology. This information, together with distributed hydrologic outputs from a model similar to GSSHA, can be an invaluable resource to decision makers during flooding events. The use of probabilistic precipitation nowcasts, and consequently probabilistic hydrologic forecasts, is a research thrust that seems to be promising.

*Acknowledgments.* The authors acknowledge the assistance of Dr. Fred Ogden of the University of Connecticut in providing the hydrologic model GSSHA and assisting in the simulation setup. The constructive comments of David Gochis of the National Center for Atmospheric Research are greatly appreciated. We acknowledge the insightful comments by an anonymous reviewer, which significantly improved the quality of the paper.

## REFERENCES

Battan, L. J., 1973: *Radar Observation of the Atmosphere*. University of Chicago Press, 324 pp.

Bedient, P. B., A. Holder, J. A. Benavides, and B. E. Vieux, 2003: Radar-based flood warning system applied to Tropical Storm Allison. *J. Hydrol. Eng.,* **8,** 308–318.

Belmans, C., J. G. Wesseling, and R. A. Feddes, 1983: Simulation model of the water balance of a cropped soil: SWATRE. *J. Hydrol.,* **63,** 271–286.

Boldi, R. A., M. M. Wolfson, R. J. Johnson Jr., K. E. Theriault, B. E. Forman, and C. A. Wilson, 2002: An automated, operational two hour convective weather forecast for the corridor integrated weather. Preprints, *10th Conf. on Aviation, Range, and Aerospace Meteorology,* Portland, OR, Amer. Meteor. Soc., 116–119.

Brooks, R. H., and A. T. Corey, 1964: Hydraulic properties of porous media. Colorado State University Hydrology Paper 3, 27 pp.

Dixon, M., and G. Wiener, 1993: TITAN: Thunderstorm Identification, tracking, Analysis and Nowcasting—A radar-based methodology. *J. Atmos. Oceanic Technol.,* **10,** 785–797.

Downer, C. W., and F. L. Ogden, 2004: GSSHA user's manual: Gridded surface subsurface hydrologic analysis, version 1.43 for WMS 6.1. U.S. Army Corps of Engineers, Engineer Research and Development Center Tech. Rep., in press.

Fulton, R. A., 1999: Sensitivity of WSR-88D rainfall estimates to the rain-rate threshold and rain gauge adjustment: A flash flood case study. *Wea. Forecasting,* **14,** 604–624.

——, J. P. Breidenbach, D. J. Seo, D. A. Miller, and T. O'Bannon, 1998: The WSR-88D rainfall algorithm. *Wea. Forecasting,* **13,** 377–395.

Green, W. H., and G. A. Ampt, 1911: Studies on soil physics: 1. Flow of air and water through soils. *J. Agric. Sci.,* **4,** 1–24.

Haverkamp, M. V., J. Vauclin, J. Touman, P. J. Wierenga, and G. Vachaud, 1977: A comparison of numerical simulation models for one-dimensional infiltration. *Soil Sci. Soc. Amer. J.,* **41,** 285–294.

Hutson, J. L., and A. Cass, 1987: A retentivity function for use in soil-water simulation models. *J. Soil Sci.,* **38,** 105–113.

Johnson, K., and Coauthors, 1998: Warning decision support system: The next generation. Preprints, *14th Int. Conf. on Interactive Information and Processing Systems (IIPS) for Meteorology, Oceanography, and Hydrology,* Phoenix, AZ, Amer. Meteor. Soc., J25–J28.

Kirkland, M.R., R. G. Hills, and P. J. Wierenga, 1992: Algorithms

for solving Richards' equation for variably saturated soils. *Water Resour. Res.,* **28,** 2049–2058.

Konrad, C. P., and D. B. Booth, 2002: Hydrologic trends associated with urban development for selected streams in western Washington. U.S. Geological Survey Water-Resources Investigations Rep. 02-4040, 40 pp. [Available online at http://water.usgs.gov/pubs/wri/wri024040.]

Lappala, E. G., R. W. Healy, and E. P. Weeks, 1987: Documentation of computer program VS2D to solve the equations of fluid flow in variably saturated porous media. U.S. Geological Survey Water Resources Investigations Rep. 83-4099, 184 pp.

Lee, J. G., and J. P. Heaney, 2003: Estimation of urban imperviousness and its impact on storm water systems. *J. Water Resour. Plann. Manage.*, **129,** 419–426.

Merz, B., and E. J. Plate, 1997: An analysis of the effects of spatial variability of soil and soil moisture on runoff. *Water Resour. Res.,* **33,** 2909–2922.

Mueller, C., T. Saxen, R. Roberts, J. Wilson, T. Betancourt, S. Dettling, N. Oien, and J. Yee, 2003: NCAR Auto-Nowcast System. *Wea. Forecasting,* **18,** 545–561.

National Research Council, 1996: *Toward a New National Weather Service: Assessment of Hydrologic and Hydrometeorological Operations and Services*. National Academy Press, 51 pp.

Ogden, F. L., 2000: CASC2D reference manual, version 2.0. Department of Civil and Environmental Engineering U-37, University of Connecticut, 83 pp.

——, and B. Saghafian, 1997: Green and Ampt infiltration with redistribution. *J. Irrig. Drain. Eng.,* **123,** 386–393.

——, and D. R. Dawdy, 2003: Peak discharge scaling in a small Hortonian watershed. *J. Hydrol. Eng.,* **8,** 64–73.

——, H. O. Sharif, S. U. S. Senarath, J. A. Smith, M. L. Baeck, and J. R. Richardson, 2000: Hydrometeorological analysis of the Fort Collins, Colorado, flash flood of 1997. *J. Hydrol.,* **228,** 82–100.

Roberts, R. D., and S. Rutledge, 2003: Nowcasting storm initiation and growth using *GOES-8* and WSR-88D data. *Wea. Forecasting,* **18,** 562–584.

Sharif, H. O., F. L. Ogden, W. F. Krajewski, and M. Xue, 2002: Numerical studies of radar-rainfall error propagation. *Water Resour. Res.,* **38,** 1140, doi:10.1029/2001WR000525.

Smith, R. E., C. Corradini, and F. Melone, 1993: Modeling infiltration for multistorm runoff events. *Water Resour. Res.,* **7,** 1219–1227.

Soil Conservation Service, 1986: Urban hydrology for small watersheds. UDSA Technical Release 55 (TR55), 164 pp.

Sun, J., and N. A. Crook, 2001: Real-time low-level wind and temperature analysis using single WSR-88D data. *Wea. Forecasting,* **16,** 117–132.

Tholin, A. L., and C. J. Keifer, 1960: The hydrology of urban runoff. *Trans. ASEC,* **125,** 1308–1379.

Tilford, K. A., N. I. Fox, and C. G. Collier, 2002: A weather radar system for urban hydrology. *Meteor. Appl.,* **9,** 95–104.

Tuttle, J. D., and G. B. Foote, 1990: Determination of boundary layer airflow from a single Doppler radar. *J. Atmos. Oceanic Technol.,* **7,** 218–232.

Wilson, J. W., and E. A. Brandes, 1979: Radar measurement of rainfall—A summary. *Bull. Amer. Meteor. Soc.,* **60,** 1048–1058.

——, N. A. Crook, C. K. Mueller, J. Sun, and M. Dixon, 1998: Nowcasting thunderstorms: A status report. *Bull. Amer. Meteor. Soc.,* **79,** 2079–2099.

Woolhiser, D. A., 1996: Search for physically based runoff model—A hydrologic El Dorado? *ASCE J. Hydraul. Eng.,* **122,** 122–129.

Zhang, Y., and J. A. Smith, 2003: Space–time variability of rainfall and extreme flood response in the Menomonee River basin, Wisconsin. *J. Hydrometeor.,* **4,** 506–517.